Anal. Methods Environ. Chem. J. 8 (1) (2025) 5-25

AMECJ

Research Article, Issue 1
Analytical Methods in Environmental Chemistry Journal
Journal home page: www.amecj.com/ir

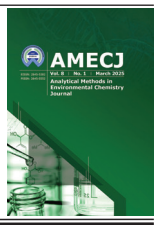

Efficient adsorption of malachite green from wastewater using agricultural biosource waste: Kinetic, isothermal, thermodynamic studies and mechanisms analysis

Smail Imame[a], Hafssa Atlas[a], Mohamed Sadoq[a], Abderahim Kali[a], Abdelouahed Amar [a] and Fatima Boukhlifi[a,*]
[a] *Laboratory of Chemistry and Biology Applied to the Environment, URL-CNRST-N◦13, Faculty of Sciences, Moulay Ismail University, Meknes 50050, Morocco.*

ARTICLE INFO:
Received 7 Nov 2024
Revised form 12 Jan 2025
Accepted 15 Feb 2025
Available online 29 March 2025

Keywords:
Malachite green,
Adsorption,
UV-Vis spectrophotometry,
Sugarcane bagasse

ABSTRACT
Adsorption on biomass has gained popularity recently as a method for reducing pollutants in wastewater before release. This work investigates the adsorption of malachite green (MG) onto sugarcane bagasse (SCB). To optimize the process, the mass of the bio-adsorbent, contact time, temperature, and pH of the MG solution were investigated with the adsorbate and the adsorbent. The observed results indicate that MG adsorption on SCB is more effective in the environment because of the electrostatic interactions between the organic cations of the dye and the negatively charged SCB surface in this pH range. In ideal circumstances, SCB removes 97% of MG. The adsorption of MG on SCB is better described by the pseudo-second-order model, according to adsorption kinetics modeling. UV-Vis spectrophotometers were used to analyze the fluids under study and determine the dye concentration. Malachite green has a limit of quantification (LOQ) of 0.1 mg L^{-1} and a limit of detection (LOD) of 0.06 mg L^{-1} using UV-Vis spectrophotometry. The measuring range of the procedure is 0.1 to 30 mg L^{-1}, which guarantees precise and repeatable results. According to adsorption isotherm modeling, the Freundlich and Langmuir models best describe MG's adsorption on SCB. Given that both the Freundlich parameter 1/n and the Langmuir separation coefficient RL are smaller than 1, it is clear that MG's bio-adsorption on SCB is beneficial. The study's findings demonstrate that SCB, an underutilized agricultural waste, is a reasonably priced bio-adsorbent with a substantial capability for treating wastewater that contains dyes.

1. Introduction

Due to various agricultural practices and industrial and domestic activities, the textile industry's intensive consumption of large quantities of water and chemicals, particularly synthetic dyes, has had a negative impact on aquatic ecosystems and the wider environment [1-3]. Dyes can be measured using UV–Vis spectrometry. The absorbance value ranges from zero to 2. When no light is absorbed, P0 equals P, and transmittance equals one. Consequently, absorption is zero. If the light absorption and transmission are 90% and 10%, respectively, resulting in T = 0.1 (absorbance =1). The resulting spectrum is a graph of absorbance against wavelength. This UV–Vis spectrophotometer range was from 200 to 800 nm. The wavelength of light that different colored

*Corresponding Author: Fatima Boukhlifi
Email: f.boukhlifi@umi.ac.ma
https://doi.org/10.24200/amecj.v8.i01.359

dyes absorb varies. Most dyes are conjugated substances with alternate double and single bonds and generally absorb light in the visible spectrum. Dyes have a narrower energy gap, and electrons are excited by lower-energy light at visible light. Measure the object's spectral reflectance before using a UV–Vis spectrophotometer to assess color. Fluorescein and indigo dye are studied using UV–Vis absorption spectroscopy [3]. Since these chemicals require treatment to lower the pollutant concentration before being released into the atmosphere, they are frequently highly harmful since they are difficult for effluents to biodegrade [4,5]. Malachite Green (MG) is a cationic dye that is extensively utilized in several industries, including the fish business, food additives, paper, leather, wool, and silk dying, as well as distilleries [6]. Although, Malachite green (MG) is harmful to the immunological and reproductive systems and can cause cancer, genotoxicity, mutagenicity, and teratogenicity in fish [6,7]. MG in any fish intended for consumption is severely prohibited in the United States and the European Council due to its excessive buildup in fish tissue [6]. Furthermore, by changing the water's color and lowering the amount of sunlight that reaches the surface, the discharge of MG into nearby waters may modify the environment. Water-soluble MG can, nevertheless, have detrimental effects even at low concentrations, including the suffocation of aquatic vegetation and the development of cancer, mutagenesis, and teratogenic effects in humans [8]. Numerous techniques, including biological treatment for biodegradable pollutants, coagulation-flocculation, electrochemical treatment, nanofiltration, ion exchange, and adsorption, can be used to remove contaminants from wastewater [9,10]. Because of the adsorption process's cost, efficiency, simplicity, and adaptability benefits are utilized increasingly frequently [11-14]. Various agricultural wastes have been employed as biosorbents for wastewater treatment. These include rice husk derivatives [15] which was used to remove crystal violet (CV), nostoc Linckia [15]which was used to remove crystal violet (CV), coffee black [16], argan shell [17]the wood powder from the shell of Argan nuts was used in raw form, or modified form by Sodium hydroxide, as a new economic and ecologic adsorbent. The effectiveness of these materials was evaluated on Methylene Blue (MB), marine macroalga sargassum muticum [18]which has prompted greater research into effective and sustainable removal techniques. Even though there have been major efforts in the previous few decades, more study is still necessary to fully examine the long-term performance and usable applicability of adsorbents and different adsorption techniques for the removal of dye. In the present study, a brown marine macroalga Sargassum muticum was used as an effective and sustainable biosorbent for the crystal violet (CV), and brown seaweed [18] which has prompted greater research into effective and sustainable removal techniques. Even though there have been major efforts in the previous few decades, more study is still necessary to fully examine the long-term performance and usable applicability of adsorbents and different adsorption techniques for the removal of dye. In the present study, a brown marine macroalga Sargassum muticum was used as an effective and sustainable biosorbent for the crystal violet (CV). The fibrous waste left behind after sugarcane is crushed to extract juice in sugar mills and refineries, known as bagasse, has been the subject of numerous scientific investigations highlighting its potential use [17,19]. The material's favorable qualities, including biodegradability, availability, buoyancy, and low cost, have shown it to be successful in eliminating pollutants from wastewater, including heavy metals and dyes. Furthermore, it mainly comprises cellulose, hemicellulose, and lignin, which have polymer structures rich in hydroxyl and carboxyl groups that interact with the chemical contaminants in the treated solution [20-22]. This work aims to investigate and examine the inherent ability of sugarcane bagasse to extract Malachite green by examining the effects of different experimental settings on the adsorption process. These parameters include mass and contact time, solution pH, and temperature. To illustrate

the feasibility of the process, thermodynamic parameters, such as enthalpy, entropy, and free energy, were determined. The thermodynamic characteristics demonstrate the spontaneous nature of the MG adsorption process on SCB.

2. Materials and methods

2.1. Materials

The dye considered in this study is a green color called malachite green or diamond green B (CAS N.: 2437-29-8, CHEMICALS, India) [23]. It was first prepared by Hermann Fischer in 1877. Its molecular structure is shown in Figure 1. It was used as supplied. The colored solutions at varying concentrations were prepared by dilution from a stock solution of 23 mg L^{-1} using distilled water. Analytical-grade chemicals were used for all experiments. Hydrochloric acid (HCl, 99% CAS N.: 7647-01-0) and sodium hydroxide (NaOH, 99%, CAS N.: 1310-73-2) were acquired from Sigma-Aldrich (Saint-Quentin-Fallavier, France).The main characteristics of the dye are described in Table 1.

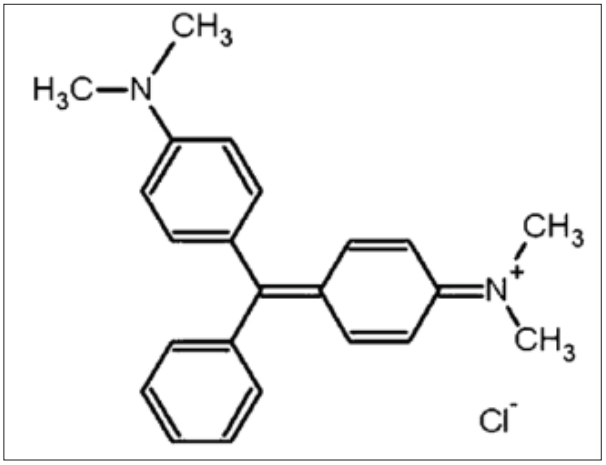

Fig. 1. The chemical structure of the MG [6].

Table 1. Physico-chemical properties of MG

Parameters	Characteristics
Molecular formula	$C_{52}H_{54}N_4O_{12}$
Molecular weight	927.03 $g.mol^{-1}$
Absorption maxima	618.0 nm
Commercial name	Malachite Green oxalate (MG) Green
Appearance	crystalline powder

2.2. Characterization Techniques

The powder X-ray diffraction patterns (XRD) of the sample were collected with a Bruker AXS model (D8-advance A25) diffractometer using Cu-K_α foundation (λ = 1.5418 Å) at 40 Kv, 20 mA, and a scan range 5–70. XRD results were recorded in the 2θ range between 2° and 70° in 0.02° angle increments. Infrared spectra were performed using a Shimizu IRAFFINIY-1S Fourier transform spectrometer (FTIR) equipped with a detector (TGS) and a ceramic source, separated by an optical system using a Michelson interferometer. The samples were prepared as 12 mm diameter pellets with a mass of 3 mg of solid diluted in 97 mg of KBr. Absorption spectra were analyzed with a resolution of 20 cm^{-1} in the wavelength range between 400 and 4000 cm^{-1}. UV-visible spectrophotometry is a qualitative and quantitative analysis method that identifies a chemical species's presence and concentration. For this purpose, the spectrophotometer used is of the type (SHIMADZU-UV 1800) that allows the measurement of the absorbance of a solution at a precise wavelength in the range between (190 to 900 nm) from the concentrations deduced from the Beer-Lambert law: $A = \varepsilon . \ell . C$.

The point of zero charge corresponds to the pH level at which the solid's surface charge becomes neutral; it was determined by the method of addition of solid [24]due to their low cost, availability, cost-effectiveness, and efficiency. In this study, we were interested in the elimination of crystal violet dye, from aqueous solutions, by adsorption on almond shell-based material, as a low-cost and ecofriendly adsorbent. The almond shells were first analyzed by Fourier transform infrared spectroscopy (FTIR). The specific surface of the solid material corresponds to its overall surface per mass unit; it was determined by the method of adsorption of methylene blue.

2.3. Preparation of the solid

Sugar cane bagasse was used as a bio-sorbent in this study. It was collected from a local vendor after the sugar cane had been crushed to extract

the sugar cane juice. It was then washed several times with water to remove dirt. The final rinses were carried out with distilled water to remove chemical residues such as salts and other soluble substances, then dried at 60°C for 24 hours. After drying, the dried sugarcane bagasse was ground using a grinder (mark: FRITSCH, Germany). They were then sieved using a sieve shaker (mark: FRITSCH, Germany), and the particle size used was determined to be less than or equal to 0.2 mm. The final product is stored for experimental studies.

2.4. Adsorption procedure

All the experiments in this work were conducted in the same experimental setup, except for the study of the effect of temperature, in which a water bath was used to set the temperature to the desired value. For this purpose, a series of samples is prepared by suspending a precise quantity in mg of the biomass in a volume of 20 mL of an aqueous solution of the green dye malachite of known initial concentration C_0 (2.5×10^{-5} M). The suspensions are then stirred for a time (t) ranging from 5 to 70 minutes. After this time, the supernatant was extracted by centrifugation. The solution was analyzed by UV-visible spectrophotometry at a wavelength of 618.0 nm. The determination of the adsorbed amounts of MG is performed from the calibration line (Scheme 1).

The adsorbed amounts are calculated using the following Equation 1.

$$q_{ads} = \frac{(C_0 - C_e),\ V}{m}$$

(Eq. 1)

Where C_0 and Ce are the initial and equilibrium concentration of the dye in mg L^{-1}, respectively; m is the mass of the solid in g; V is the volume of the dye solution MG in L, and quads is the adsorbed amount per gram of adsorbent in mg g^{-1}.

2.5. Modeling of adsorption kinetics

To interpret the MG adsorption on SCB experimental data. Three kinetic models were utilized: intra-particle diffusion, pseudo-second-order (PSO), and pseudo-first-order (PPO).

2.5.1.Pseudo-first-order model

The pseudo-first-order model is given by Lagergren, which is expressed by the following Equation 2 [25].

$$\frac{dqt}{dt} = K_1(q_e - q_t)$$

(Eq. 2)

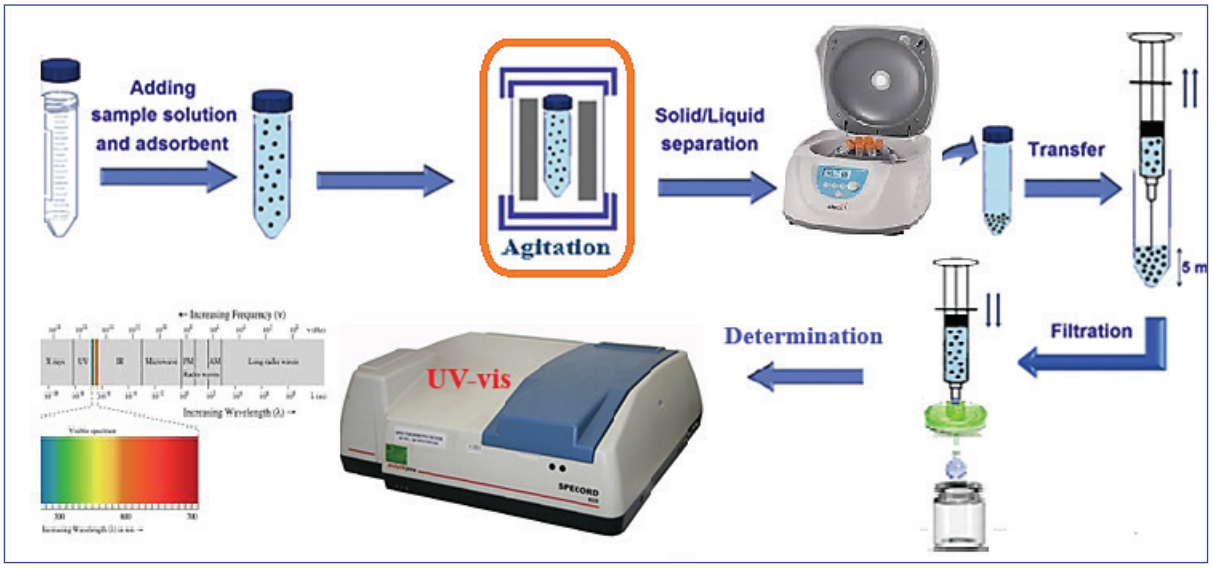

Scheme 1. Procedure for separating MG on SCB by UV-visible.

Where k_1 is the first order reaction rate constant of adsorption of MG on BCS in (min^{-1}), q_e, q_t the amount of MG adsorbed at equilibrium and at time t in (mg g^{-1}), t the contact time in (min).
After integration with initial conditions q_{t0} at t = 0, Equation 3 was obtained. For the representation of Log (qe-qt) = f(t), we obtain a line that gives k_1 and qe.

$$q_t = q_e(1 - e^{K_1 t})$$

(Eq. 3)

2.5.2. Pseudo-second order model

The following expression gives the pseudo-second-order model in Equation 4 [26].Where K_2 is the second-order reaction rate constant of adsorption of MG on SCB in ($g.mg^{-1}.min^{-1}$).

$$\frac{dqt}{dt} = K_2(q_e - q_t)^2$$

(Eq. 4)

After integration of Equation 4, we obtain Equation 5. The linearization of the Equation 5 gives Equation 6.

$$q_t = \frac{K_2 q_e^2 t}{K_2 q_e t + 1}$$

(Eq. 5)

$$\frac{t}{q_t} = \frac{1}{K_2 q_e^2} + \frac{1}{q_e} t$$

(Eq. 6)

The representation of t/qt = f(t) allows us to obtain a line from which we determine k_2 and q_e.

2.5.3. Intra-particle diffusion model

The intra-particle diffusion is described by Equation7 by Weber and Morris [27]. The K_d is the intra-particle diffusion rate constant in (mg g^{-1} $min^{0.5}$), and C is the boundary layer thickness in (mg g^{-1}). In Equation 7, the representation of qt = f ($t_{1/2}$) (allows to calculate k_d and C.

$$q_t = K_d t^{1/2} + C$$

(Eq. 7)

2.6. Thermodynamic parameters

The thermodynamic parameters (ΔG°), (ΔH°), and (ΔS°) for the studied system (MG/SCB) were determined and calculated at different temperatures (25°C, 35°C and 45°C). The adsorption-free energy (ΔG°) is calculated according to the standard Gibbs formula defined by Equation 8.

$$\Delta G° = - RT \ln (K_d),\ K_d = \frac{q_e}{Ce}$$

(Eq. 8)

q_e (mg g^{-1}) represents the amount of adsorbed dye at equilibrium, and Ce (mg L^{-1}) is the residual concentration of the adsorbate at equilibrium.
Also, the thermodynamic parameters of adsorption of the MG on the adsorbent can be estimated from the curve representing the variation ln (K_d) as a function of 1/T, which was shown in Equation 9.

$$\ln K_c = \frac{\Delta S^\circ_{ads}}{R} - \frac{\Delta H^\circ_{ads}}{RT}$$

(Eq. 9)

The values of (ΔH°_{ads}) and (ΔS°_{ads}) are calculated from the slope and intercept of the line obtained by plotting ln (K_c) versus $\frac{1}{T}$, respectively.

2.7. Modeling of adsorption isotherms

2.7.1. Langmuir Isotherm Model

The Langmuir model was initially employed for systems featuring monolayer adsorption occurring on the surface of the adsorbent. This model assumes that all adsorption sites are identical, do not depend on surface coverage, and take place without lateral interaction with the adsorbate molecules. The following Equation 10 represents this model. In equation 10, qm is the maximum

adsorbed quantity in mg g^{-1}, and K_l is the Langmuir constant in L mg^{-1}. To determine the adsorption parameters of this model, we use the linear form of the Langmuir isotherm, represented by Equation 11. In addition, among the essential characteristics of the Langmuir isotherm is the separation factor $R_{L,}$ defined by Equation 12.

$$q_e = \frac{q_m.K_l.C_e}{1+K_l.C_e}$$

(Eq. 10)

$$\frac{1}{qe} = \frac{1}{K_l.q_m.C_e} + \frac{1}{q_m}$$

(Eq. 11)

$$R_l = \frac{1}{1+K_l.C_e}$$

(Eq. 12)

With: C_i is the initial concentration of the dye (mg L^{-1}) and K_L the Langmuir constant (Lmg^{-1}). Values of R_L indicate the shapes of isotherms to be either unfavorable ($R_L > 1$), linear ($R_L = 1$), favorable ($0 < R_L < 1$) [28].

2.7.2. Freundlich Isothermal Model

The Freundlich empirical model is founded on adsorption on heterogeneous surfaces and is represented by Equation 13. The linearization of this equation implies a passage of the terms in logarithmic form.

$$\text{Log}\,(q_e) = \text{Log}(K_f) + \frac{1}{n}\text{Log}(C_e);\ \ q_e = K_F.\ C_e^{1/n}$$

(Eq.13)

Where qe is the amount adsorbed at equilibrium, C_e is the residual concentration of the dye at equilibrium, and n represents the adsorption intensity and indicates whether the adsorption is favorable. If n<1 linear adsorption, if n>1 physical adsorption is favorable [29]. the linear form of the isotherm by plotting Log qe = f(LogCe).

2.7.3. Temkin Isothermal Model

The Temkin isotherm is derived assuming that the decline in adsorption heat follows a linear trend, unlike the logarithmic decrease presumed by the Freundlich equation. Generally, the Temkin isotherm is expressed by Equation 14 [30].

$$q_e = \frac{R.T}{b_T}.\ \text{Ln}(A_T.C_e)$$

(Eq.14)

The b_T and A_T are Temkin isotherm constants, R is the perfect gas constant (8.314 $KJmol^{-1}$), Ce is the equilibrium concentration of dye ions (mg L^{-1}), and T is the absolute temperature.

3. Results and discussion

3.1. Characterizations

3.1.1. XRD Analysis

The XRD diffractogram of sugarcane bagasse is shown in Figure 2. The SCB is mainly composed of lignin, cellulose, and hemicelluloses. The two peaks detected have values of 2ɵ around 16 and 22 due to the semi-crystalline structure of the cellulose contained in the biomass [31]. Moreover, the XRD spectrum resembles that of other lignocellulosic residues [32].

3.1.2. FT-IR analysis

Fourier transform infrared spectroscopy was utilized to analyze the SCB solid, and the resulting FT-IR spectrum is presented in Figure 3. The FT-IR spectra of BCS show the presence of many functions on the surface of the adsorbent such as: The strong band appearing at 3374 cm^{-1}, is attributed to OH groups (alcohols, phenols, and carboxylic acids) [33,34]. The band at 1732 cm^{-1} is characteristic of the stretching vibration of the C=O of xylan carboxylic acids present in hemicelluloses [23].The bands at 1611 cm^{-1} ant 1640 cm^{-1} is attributed to the C=C deformation (aromatic of lignin) [35], thus the band at 1370 cm^{-1} confirms

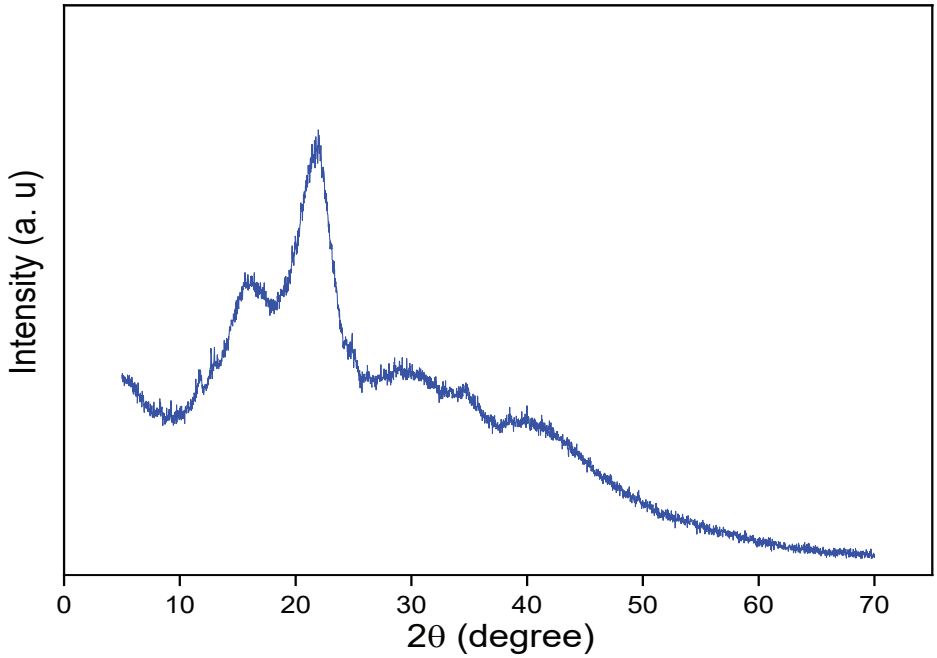

Fig. 2. Powder XRD patterns of SCB.

the presence of methoxy -C-O groups of lignin [36], the bands at 1250 and 1052 cm^{-1} are attributed to the stretching vibration of the C-O bonds of the aromatic compounds and the acid, alcohol, phenol, ether, and ester functions [33],830 cm^{-1} due to the vibration of the aromatic C-H bond, corresponding to the polysaccharides and lignin [37], and the band appears at 606 cm^{-1} due to the elongation of the C-X bond (alkyl halide) [33].

3.1.3.Point of zero charge

In this work seven vials were prepared, each containing 50 ml of sodium chloride NaCl (10^{-3} M). The pH of these vials is adjusted to the initial pH (values between 2 and 12) by adding NaOH or HCl solution (0.1M). After the initial pH adjustment, 100 mg of the solid was added to each vial. The suspensions were kept under stirring, at room temperature, for 24 h, and the final pH was measured.

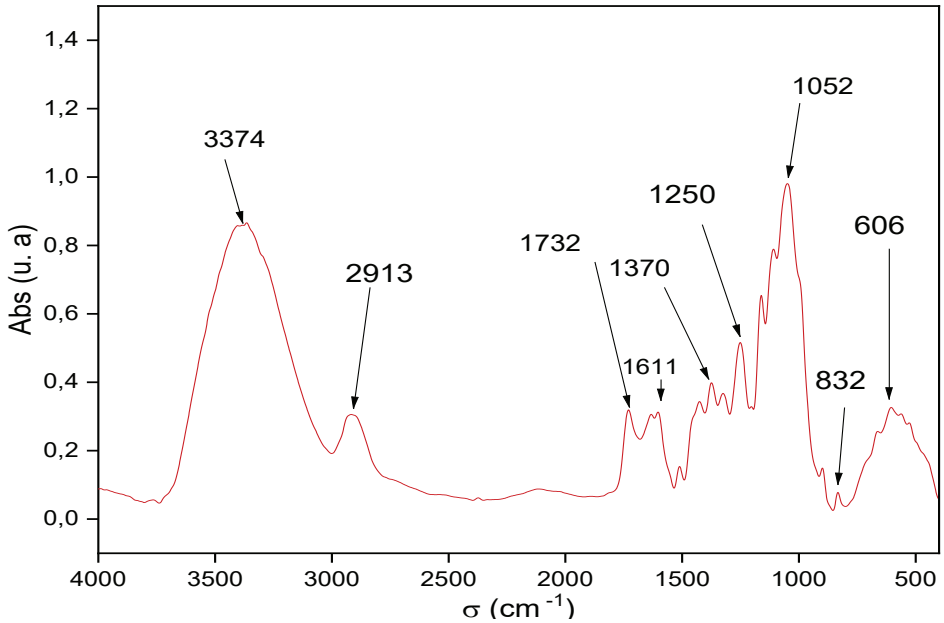

Fig. 3. FT-IR spectra of the BCS solid

The representation of ΔpH = f(pHi) a determines the pH_{pzc} value. The latter results from the intersection of the curve with the x-axis [38]. The representation of ΔpH = f(pHi) a allows us to determine the value of pHpzc, which is ulster in Figure 4. It shows that the pH value at which the solid surface has zero charge corresponds to pH = 7.3, so the solid surface is opposing at pH > 7.3 and positive below pH = 7.3.

3.1.4.Determination of the specific surface

The specific surface area of SCB was determined by the methylene blue adsorption method, which consists in studying the adsorption of methylene blue. A precise mass in mg of the biomass was suspended in a volume of the aqueous solution of methylene blue of known initial concentration, and the kinetics of the process were followed until a maximum value of the adsorption capacity was obtained. The specific value is calculated by Equation 15 [39]. The value of S_{BM} was obtained at 28.44 $m^2 g^{-1}$.

$$S_{BM} = q_m.N_A.S \quad (Eq.15)$$

With SBM: specific surface determined by BM adsorption (m^2g^{-1}); qm: maximum adsorbed quantity (mol g^{-1}); S: the surface of a BM molecule (175 $Å^2$); N_A: Avogadro number.

3.2. Study of MG adsorption on BCS

Various parameters influencing the adsorption phenomenon are examined: the mass of the adsorbate, the solution's initial pH, the adsorbent-adsorbate contact time, and the solution temperature.

3.2.1.Effect of adsorbent mass.

Different adsorbent masses ranging from 0.01 to 0.1 g are added to individual 20 mL samples of an aqueous solution containing 2.5×10^{-5} M of the dye to determine the optimal quantity of adsorbent required to remove the highest amount of dye. The solution is then stirred magnetically for 60 minutes until the adsorption equilibrium is reached. The findings of this experiment are presented in Figure 5. Also, Figure 5 shows that the percentage of dye removal increases with the mass of the bio-adsorbent and a stabilization of the adsorption rate beyond a mass of 50 mg, which indicates that the adsorption equilibrium is reached from 50 mg of adsorbent (saturation). An optimal amount of 50 mg of biomass will be necessary to fix the maximum amount of the dye, corresponding to the removal of 97%.

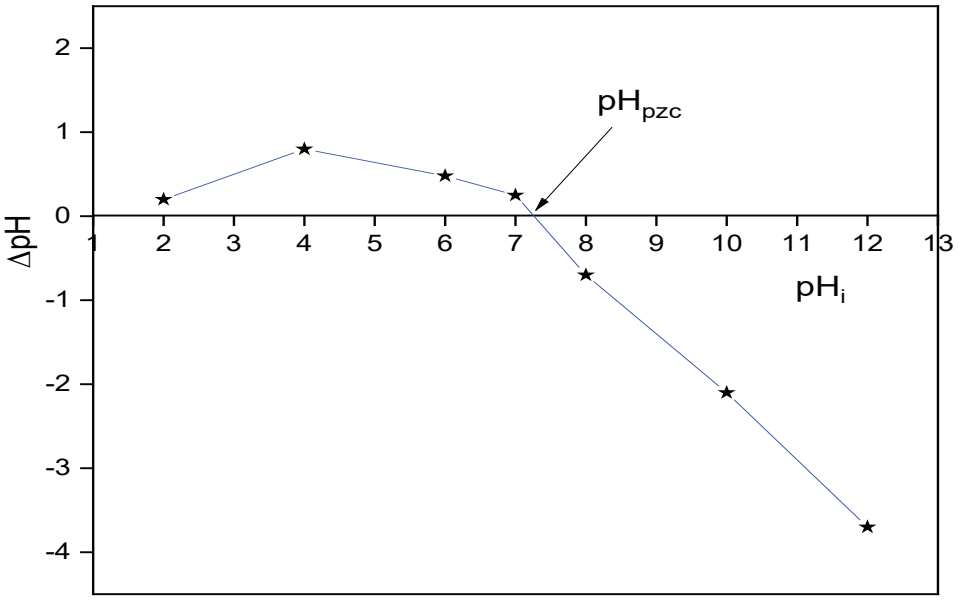

Fig. 4. Point of zero charge of BCS

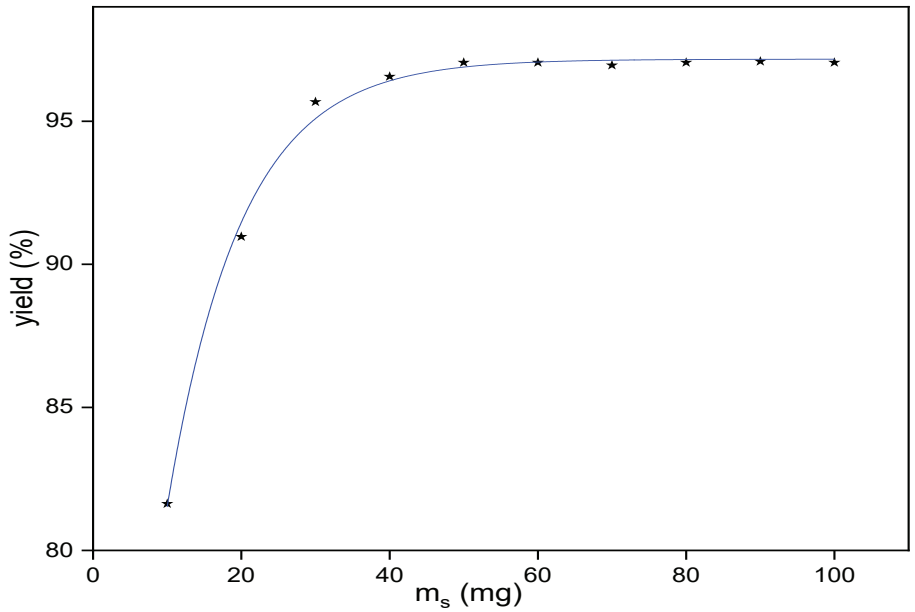

Fig. 5. Percentage of MG removal as a function of bagasse mass.

3.2.2.Effect of temperature

In order to determine the optimal temperature that gives highest capacity of adsorption, studies were done in a water bath at temperatures 25, 30, 35, 40, and 45°C by adding 50 mg of the bagasse in 20mL of the GM solution of a concentration of 2.5 $\times 10^{-5}$M, for one hour under stirring. The results obtained are shown in Figure 6 below. The resulting curve indicates that when temperature increases from 25 to 45°C, the MG adsorption capacity decreases from 12.84 to 12.50 mg g^{-1}. This result, in line with Arrhenius' law, implies that the surface reaction is exothermic and that the contact between the dye molecules and the biosorbent's active sites decreases with increasing temperature, which is detrimental to the adsorption process [40]. The best results are obtained at room temperature.

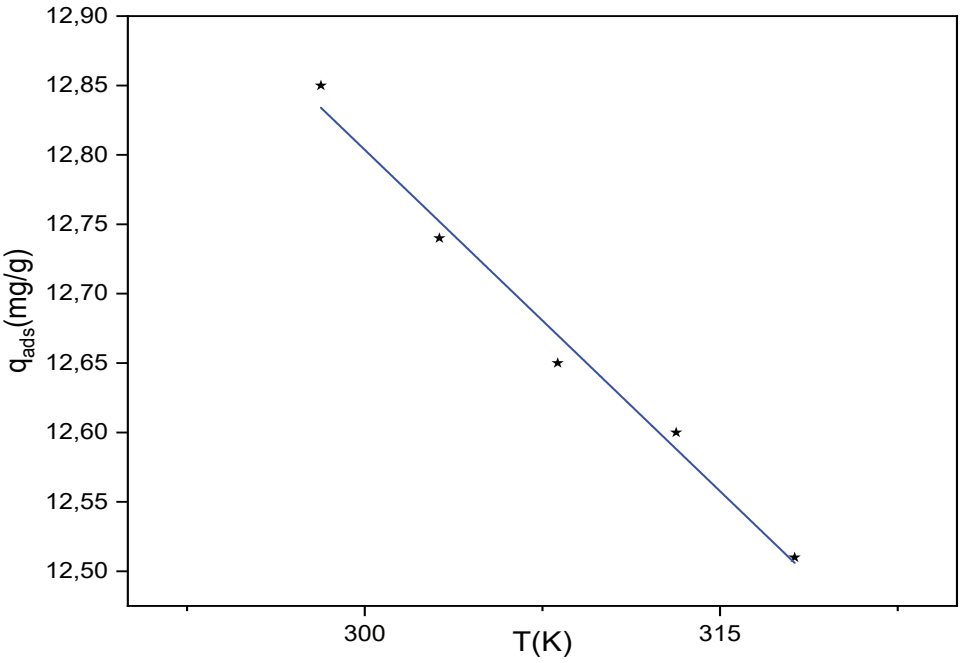

Fig. 6. Influence of the temperature on the amount of adsorbed dye.

3.2.3.Effect of contact time

To determine the time required for saturation of the adsorbate by the adsorbent/maximum retention of the dye, volumes of 20 mL of the dye solution at a concentration of 10^{-4} mol L^{-1} are mixed with 50 mg of the biomass at the following temperatures 25, 35 and 45°C. The whole is stirred at times ranging from 5 to 70 minutes. Separation was performed by centrifugation of the suspension. The residual concentrations were determined using the UV-VIS spectrophotometer at 618 nm. The results are shown in Figure 7. The figures show that the amount of MG adsorbed by biomass adsorbent at different temperatures increases over time until an equilibrium plateau is reached, after 50 minutes. This is because the adsorbent's surface initially has active sites available for use. After this time (the equilibrium time), there is a decrease in adsorption efficiency because fewer free sites remain on the adsorbent's surface [24]. Additionally, the graphs demonstrate that the quantity of MG adsorbed by the biomass is somewhat temperature-sensitive. Raising the temperature has a negative effect on adsorption, indicating an exothermic process. Notably, this adsorption happens quickly, taking place in the first forty minutes after adsorption begins.

3.2.4.Effect of pH

Several tests were conducted to evaluate the effect of the reaction media's pH on the adsorbent's ability to adsorb dye. This required putting biomass suspensions in 20 milliliters of dye solution and changing the pH between 2 and 12 during 50 minutes of contact. By adding 0.1M of HCl or 0.1M of NaOH, the suspensions' pH was brought to the required level. Figure 8 displays the results of varying the adsorption percentage about the solution's pH. The graph shows the significant impact of the character of the mixture on the adsorption of MG by the adsorbate. As a result, effective dye retention is observed over a pH range from 8 to 10, with particularly remarkable performance at pH 10. Above this pH range, a decrease in retention efficiency is observed. To explain the effect of solution pH on these interactions, the pH value of the zero charge point pHpzc was used. Since the pHpzc of the solid used is 7.3, the surface of the adsorbent is positively charged when the pH of the solution is below this value and is negatively charged when the pH of the solution is above this value. As the dye used is cationic, its dissolution releases positively charged ions, so hydrophobic and chemical interactions could be the main

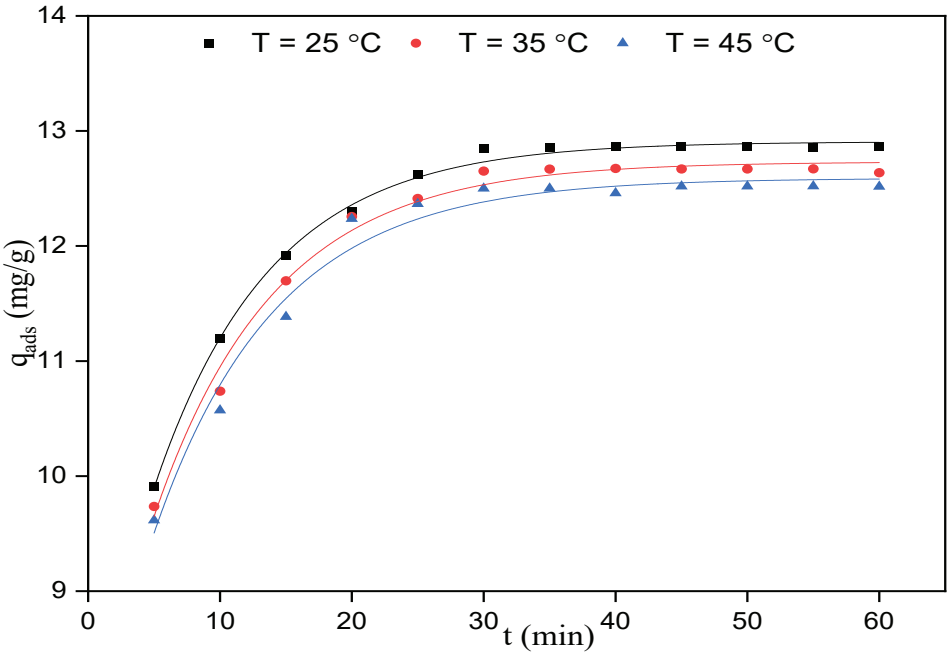

Fig. 7. Effect of contact time.

adsorption forces in the pH range below pHpzc. The significant retention of the dye at pH values above pHpzc can be explained by electrostatic interactions between the different charges in the suspension and the surface of the adsorbent. In addition, MG molecules (pka = 10.3) [6] are protonated in the acid medium and deprotonated at higher pH values, which explains the decrease in dye retention at pH values above 10.

3.3. Thermodynamics parameters

Figure 9 shows the evolution of $\ln(K_c)$ as a function of $\frac{1}{T}$. The activation energy of the adsorption process is determined by applying the Arrhenius equation of $k = A.e^{-Ea/RT}$. The thermodynamic parameters are grouped in Table 2. The results confirm the exothermic nature of MG's adsorption onto the adsorbent ($\Delta H°$ is negative). A decrease in disorder during the adsorption of MG onto the adsorbent is

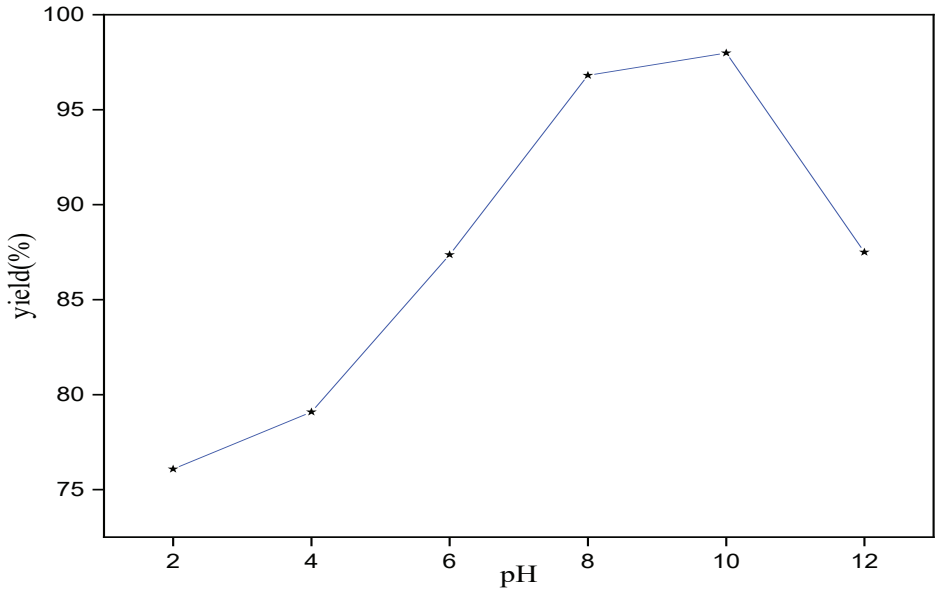

Fig. 8. Influence of pH on MG adsorption

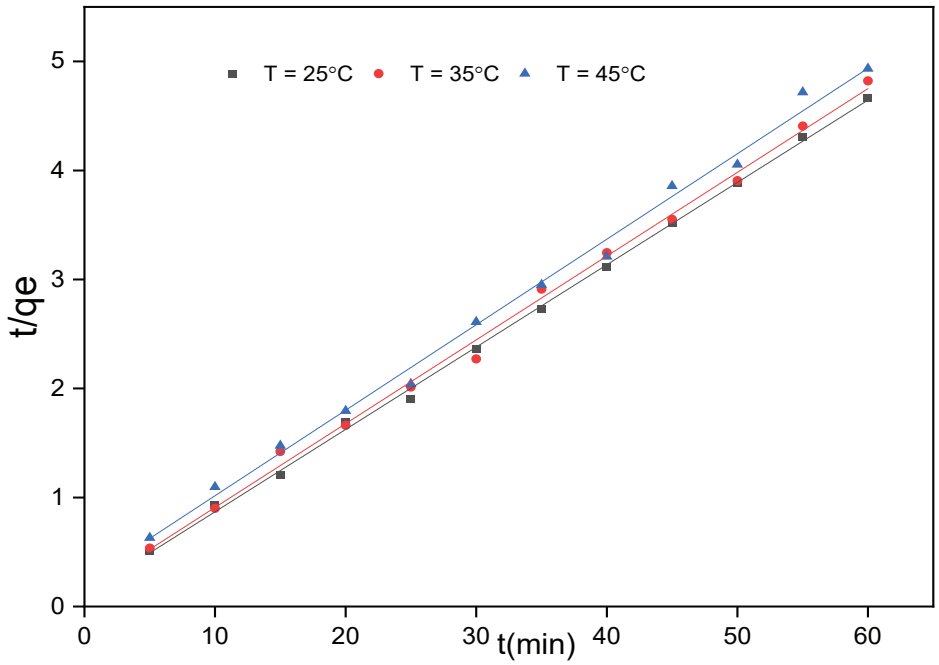

Fig. 9. Evolution of $\ln(K_c)$ as a function of T^{-1}

Table 2. The thermodynamic parameters

Temperature (°K)	$\Delta H°_{ads}$ (Kj mol^{-1})	$\Delta S°_{ads}$ (jK^{-1} mol^{-1})	$\Delta G°_{ads}$ (Kj mol^{-1})	R^2	Ea (Kj mol^{-1})
298			-26.046		
303			-26.048		
308	-25.90	0.49	-26.051	0.998	35.75
113			-26.053		
318			-26.056		

indicated by the negative values of ΔG° and ΔS°, which indicate that the process is spontaneous [41]. The Arrhenius equation was also used to compute the activation energy value, which is less than 40 kj mol^{-1}. This suggests that a physisorption mechanism underlies the adsorption process.

3.4. Modeling of adsorption kinetics

3.4.1. Pseudo-first-order kinetics

The figure shows the results of these models, with the kinetic parameters derived from the slopes and intercepts of the theoretical lines. Table 3 shows the kinetic parameters derived from the linear Lagergren models. The obtained data (Figure 10 and Table 3) demonstrate that the experimental points for this model are not entirely linear, the experimentally adsorbed quantities of malachite green are significantly different from the calculated qcal, and the R^2 coefficients depart considerably from the value of 1. As a result, this model cannot explain the outcomes of the adsorption of malachite green on our adsorbent.

3.4.2. Pseudo-second order kinetics

The experimental results were also compared with the pseudo-second-order kinetic model Figure 11. The results obtained for the linear adsorption kinetics models are shown in the figure 11.

Table 3 shows the kinetic parameters calculated from the slopes and ordinates of the theoretical lines. According to Figure 11, the model with the highest correlation factor is the pseudo-second-order model. The adsorbed quantity values in this model q_{cal} are similar to those obtained experimentally q_{exp}, with correlation coefficients R^2 close to 1. In this way, it can be concluded that the pseudo-second-order model better represents the malachite green adsorption process on the SCB solid. It would appear that the biosorption of MG molecules by the SCB from an aqueous solution proceeds rapidly [42]. This result is similar to that observed in other research [6].

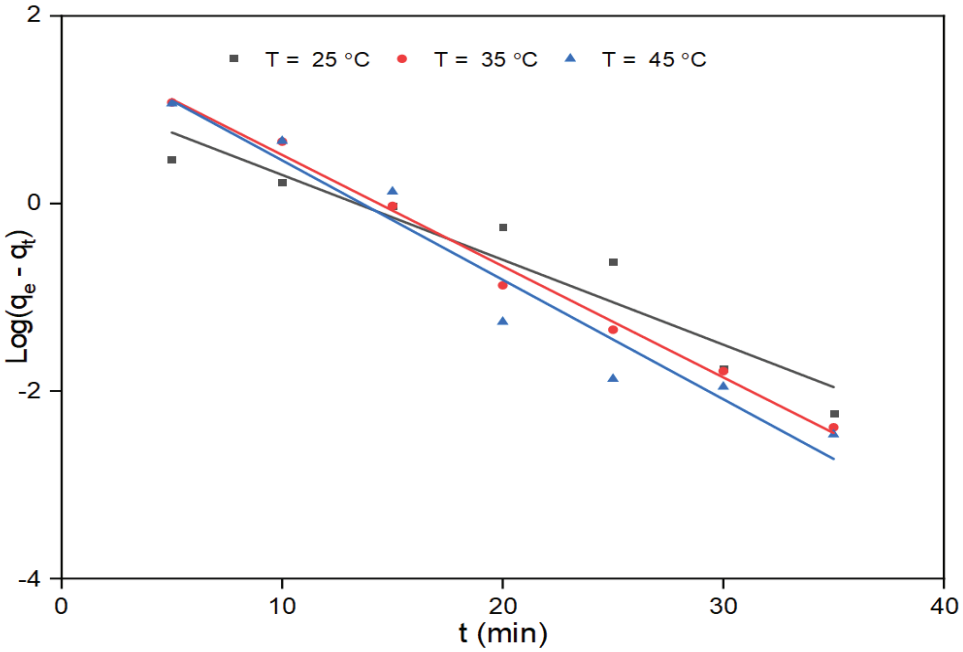

Fig. 10. Application of the pseudo-first-order model on MG-SCB adsorption

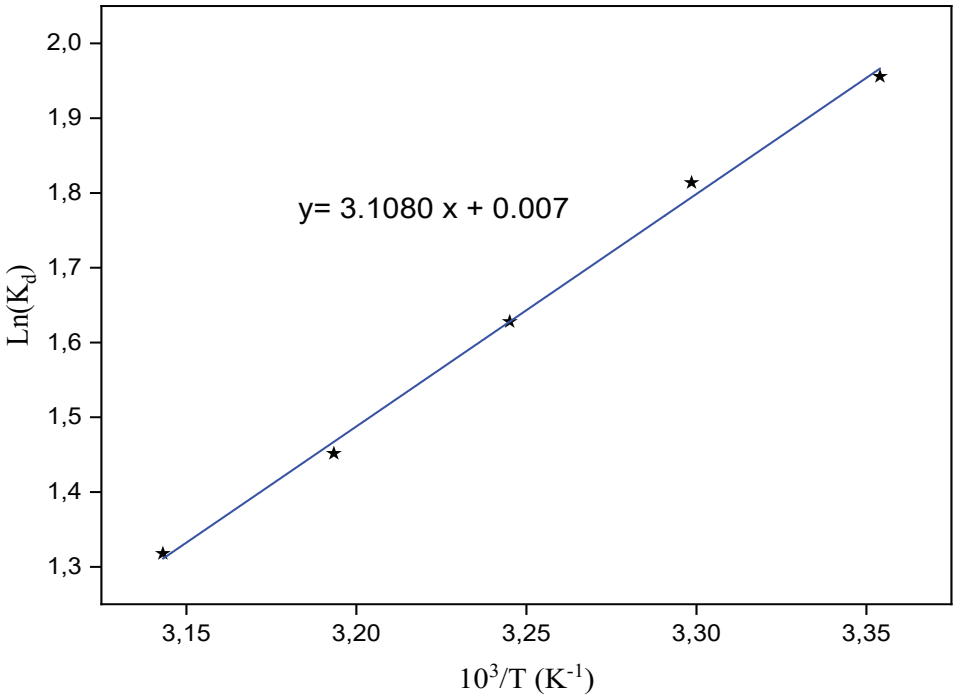

Fig. 11. Application of the pseudo-second-order model on GM-BCS adsorption.

3.4.3.Intra-particle diffusion model

Figure 12 below shows a graphical representation of the variation of the amount of dye adsorbed at each time qt as a function of the square root of time ($t_{1/2}$). According to these results, the curves representing qe = f ($t^{0.5}$) do not pass through the origin, which indicates that the diffusion of the dyes into the biomass pores is not the only mechanism determining the adsorption kinetics, the double linearity of the curves suggests that there is a combination of two different steps. Therefore, the rate of adsorption kinetics varies from one step to the other. Table 4 displays the parameters of the intra-particle diffusion model for the adsorption of MG on SCB. From these results, it can be seen that the diffusion rate constant Kd values in the first step are higher than those in the second step, which indicates that the first step of the dye diffusion kinetics is faster than the second step. The first step represents the dyes' diffusion on the adsorbent's external surface. In contrast, the second step reflects the diffusion of the dye molecules through the internal pores within the biomass particles, which is a slower step [43]. Thus, the values of the constant C are different from 0; this last one expresses the thickness of the diffuse layer; we notice that the intra-particle diffusion is not the only factor that controls the rate of adsorption of malachite green on the adsorbent [44]. Table 4. Parameters of the intra-particle diffusion model of MG on BCS.

Table 3. Kinetic parameters of linear modeling of MG dye adsorption.

Temperature	Adsorbed values	Pseudo-first order model			Pseudo-second order model		
(°K)	q_{exp}(mg.g^{-1})	q_{cal}	K_1	R^2	q_{cal}	K_2	R^2
298	12.86	3.54	2.21	0.914	12.50	0.049	0.999
308	12.66	0.1	2.81	0.866	12.50	0.082	0.998
318	12.51	0.01	0.48	0.965	12.50	1.28	0.999

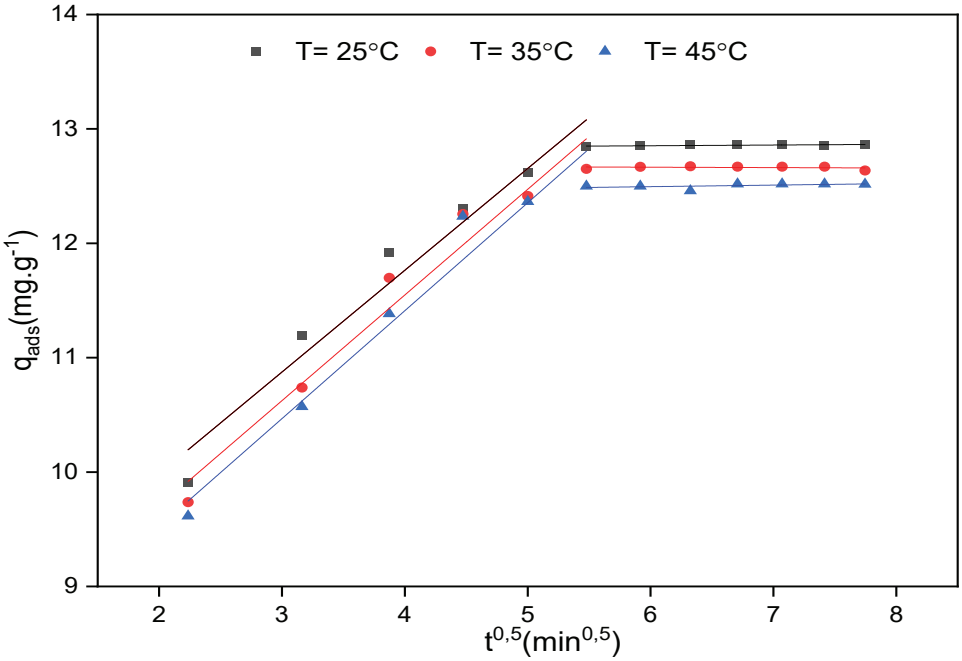

Fig. 12. Application of the external diffusion model to adsorption MG -SCB

According to these results, the curves representing qe = f ($t^{0.5}$) do not pass through the origin, which indicates that the diffusion of the dyes into the biomass pores is not the only mechanism determining the adsorption kinetics, the double linearity of the curves suggests that there is a combination of two different steps. Therefore, the rate of adsorption kinetics varies from one step to the other. Table 4 displays the parameters of the intra-particle diffusion model for the adsorption of MG on SCB. From these results, it can be seen that the diffusion rate constant Kd values in the first step are higher than those in the second step, which indicates that the first step of the dye diffusion kinetics is faster than the second step. The first step represents the diffusion of the dyes on the external surface of the adsorbent, while the second step reflects the diffusion of the dye molecules through the internal pores within the biomass particles, which is more of a slow step [43]. Thus, the values of the constant C are different from 0; this last one expresses the thickness of the diffuse layer; we notice that the intra-particle diffusion is not the only factor that controls the rate of adsorption of malachite green on the adsorbent [44].

3.5. Modeling of adsorption isotherm

3.5.1.Langmuir Isotherm

Figure 13 illustrates the modeling results obtained from the model, while Table 5 summarizes the isotherm's parameters. The data presented in Table 5 shows that the experimental data for MG biosorption on biomass is well described. This is confirmed by the high value of the coefficient of determination (R^2 = 0.98), proving that the biosorption process occurred in a monolayer fashion. In addition, MG dye ions (KL = 0.011 L mg^{-1}) highly refined the biosorption sites on the biomass surface, demonstrating their ability to effectively

Table 4. Parameters of the intra-particle diffusion model of MG on BCS.

Temperature	1st right			2nd right		
(°K)	C	K_1	R^2	C	K_2	R^2
298	0.92	2.23	0.917	12.45	0.057	0.65
308	0.95	2.54	0.94	12.29	0.06	0.58
318	0.96	2.53	0.969	12.01	0.07	0.807

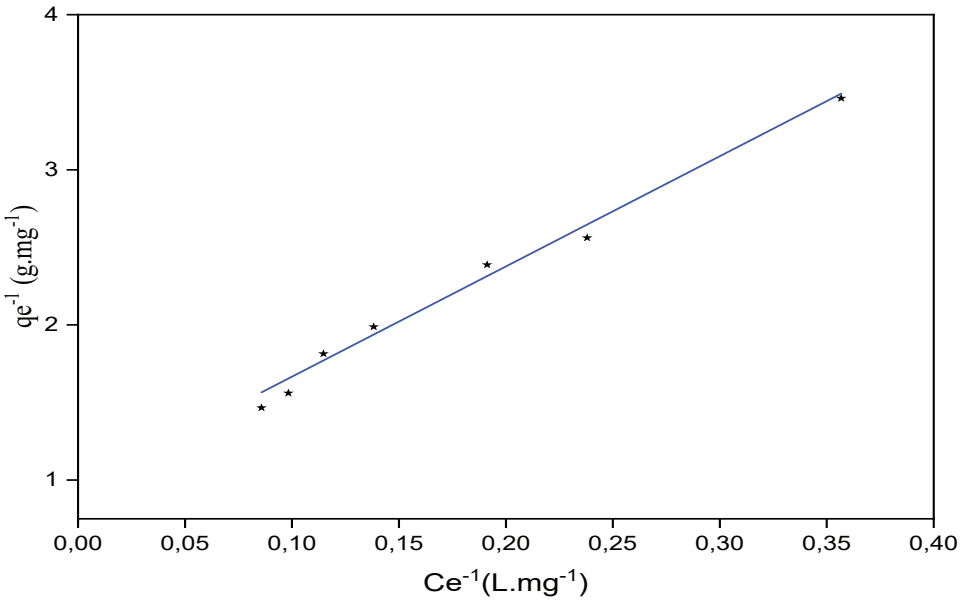

Fig. 13. Linear representation of the Langmuir model of MG adsorption on SCB

remove dye particles from aqueous solutions [18]. Deviations from the linearity of biosorption are considered when determining the Langmuir isotherm model's second parameter (dimensionless factor RL). The value of R_L is between zero and one, indicating favorable biosorption [28]. Furthermore, the maximum dye adsorption amount predicted by this model, qm, closely matches the experimental value (q_{exp}:12.84 mg g^{-1}).

3.5.2. Freundlich isotherm

The outcomes of modeling the adsorption isotherm of the dye on the adsorbent are depicted in the following Figure 14, based on this model. According to Sahu and colleagues [45], it has been reported that the higher the value of n, the more intense the reaction between the adsorbate and the biosorbent. In addition, the increase in the R^2 value (0.98) indicates that multilayer biosorption has an impact on the process. This also shows that the Freundlich isotherm model accurately illustrates the equilibrium of MG biosorption by SCB biomass, with a high affinity between the heterogeneous biomass surface and the MG particles [45].

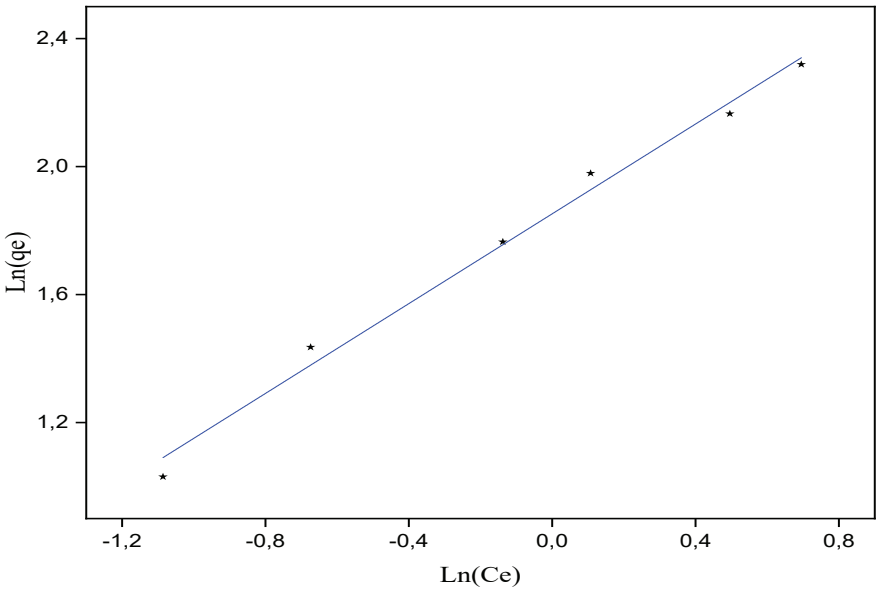

Fig. 14. Linear representation of the Freundlich model of MG adsorption on SCB

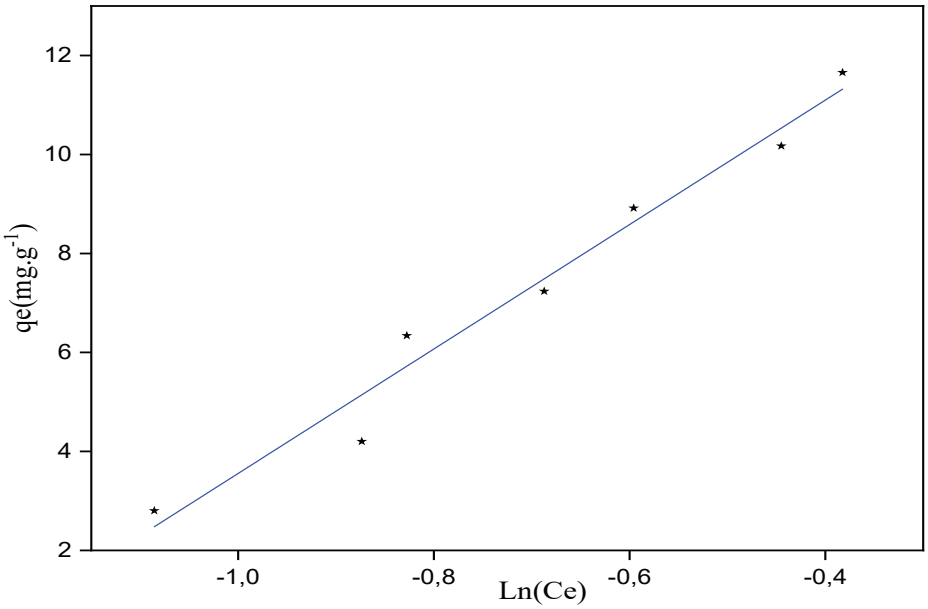

Fig. 15. Linear representation of the Temkin model of MG adsorption on SCB

3.5.3. Temkin isotherm

Figure 15 depicts the outcomes of modeling the dye's adsorption isotherm on the adsorbent, as per this model. According to the results in Table 5, the Temkin model is suitable for the biosorption of MG on biomass, as demonstrated by the high R^2 value (0.97). This also confirms the possibility of heterogeneous sites with different binding energies [46]. The higher b-value (187.1 $Jmol^{-1}$) suggests a strong interaction between MG ions and different functional groups present on the biomass surface, which is associated with the decrease of the adsorption heat of ions in the layer [18]. Furthermore, the adsorption energy of the dye from the aqueous solution, according to the Temkin model (b_T), is positive, suggesting an exothermic nature of the adsorption [47]. According to the Langmuir, Freundlich, and Temkin biosorption isotherms, the R^2 values are all greater than 0.97, which suggests that the biosorption process is multimechanistic and that it is very likely to be a multilayer physisorption.

Table 5. Parameters related to the adsorption models used.

Isotherm	Parameters
Langmuir	$q_m = 12.9$ $K_L = 0.011$ $R_L = 0.8$ $R^2 = 0.98$
Freundlich	$K_F = 2.752$ $\frac{1}{n} = 0.69$ $R^2 = 0.98$
Temkin	$A_T = 1.15$ $b_T = 187.1$ $R^2 = 0.97$

3.6. Mechanism of MG adsorption on SCB

To propose a mechanism for MG adsorption on SCB, Fourier transform infrared spectroscopy is a critical study that must be conducted. This examination is an essential tool for examining the interaction between dye molecules and the solid material's surface-active sites, and it is carried out both before and after MG adsorption. Comparison of the two FTIR spectra (Fig. 16) reveals neither the appearance of new bands nor the disappearance of bands previously observed in the raw SCB alone. The only change detected is a variation in the intensity of the absorption bands. Indeed, there is a reduction in the intensity of the broadband located between 3374 cm^{-1}, corresponding to the elongation of the vibrations of the (OH) groups, suggesting a possible involvement of hydrogen bonds between the hydroxyl groups on the SCB surface and the nitrogen atoms of the MG in the adsorption mechanism. In addition, ion exchange could occur by replacing the sodium, magnesium, and calcium ions present on the biomass cell wall with ions from the MG dye [18]. This would also be a process of electrostatic interaction, as the biosorbent surface is negatively charged at a pH above 7.3 (pH_{pzc}); this facilitates the interaction of the algal surface with the positively charged particles of the MG dye (Schema 2). Thus, it can be concluded that hydrogen bonding, ion exchange, and electrostatic interaction may all play a role in the biosorption of MG dye on SCB biomass.

4. Conclusion

The study focused on using SCB sugar cane bagasse waste in its natural form to remove the malachite green (MG) dye by adsorption in an aqueous medium. The physicochemical characterization of the material has shown that it is rich in hydroxyl groups present in several surface functions, such as acids and alcohols. The specific surface of the adsorbent is estimated at around 28.44 m^2g^{-1}. This surface is opposing at a pH greater than 7.3; the biosorbent is rich in oxygenated functions such as alcohol, acid, and ether, capable of attracting cationic pollutants in an essential medium. UV-Vis spectrophotometry is used to assess the concentrations of MG dye solutions. The performance of BCS in removing MG from wastewater was about 12.84 mg g^{-1}, corresponding to a removal efficiency of 97% at room temperature. The study of the optimization of the conditions showed that the adsorption capacity decreases with the increase in temperature, which represents a strong point for treating this dye. The kinetic and isothermal study results clearly showed that the adsorption of MG on the biosorbent adhered to the pseudo-second-

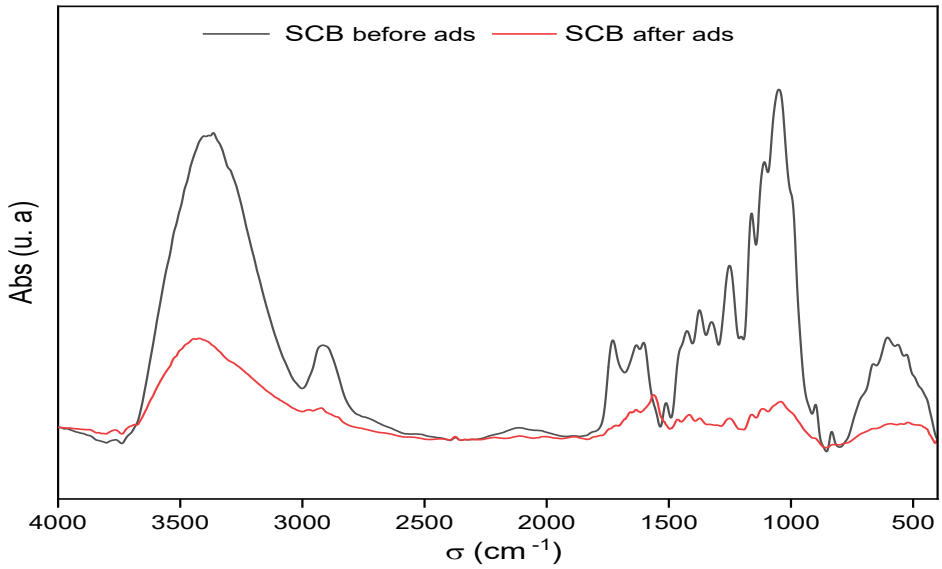

Fig. 16. FT-IR spectra of SCB before and after adsorption of dye molecules.

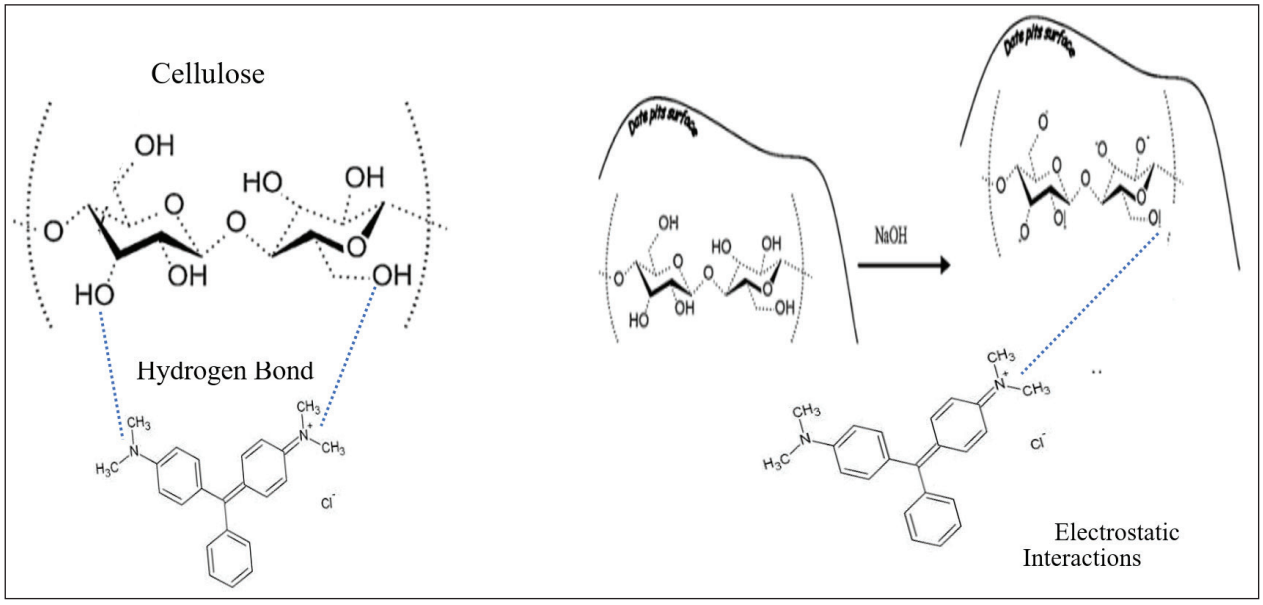

Scheme 2. Proposed mechanism for the retention of MG dye over the SCB solid

order model. The variations in adsorption and Gibbs free energy (ΔG°), entropy (ΔS°), and enthalpy (ΔH°) were computed, revealing that the adsorption of MG occurs spontaneously through an exothermic process. The investigation into the adsorption of MG has shown that this material constitutes an adsorbent abandonment and is economical and practical for the treatment of wastewater loaded with dyes.

5. Acknowledgements

The authors thank the Applied Chemistry and Biology Laboratory, Faculty of Sciences, Moulay Ismail University, Morocco.

6. References

[1] S. Teimoori, H. Shirkhanloo, A. H. Hassani, M. Panahi, N. Mansouri, Rapid extraction of BTEX in water and milk samples based on functionalized multi-walled carbon nanotubes by dispersive homogenized-micro-solid phase extraction, Food Chem., 421 (2023) 136229. https://doi.org/10.1016/j.foodchem.2023.136229

[2] S. Teimoori, H. Shirkhanloo, A. H. Hassani, M. Panahi, N. Mansouri, An immobilization of aminopropyl trimethoxysilane-phenanthrene carbaldehyde on graphene oxide for toluene extraction and separation in water samples, Chemosphere, 316 (2023) 137800. https://doi.org/10.1016/j.chemosphere.2023.137800

[3] M. Arjomandi, A Review: Analytical methods for heavy metals determination in environment and human samples, Anal. Methods Environ. Chem. J., 2 (2019) 97–126. https://doi.org/10.24200/amecj.v2.i03.73

[4] M. B. H. Abadi, H. Shirkhanloo, J. Rakhtshah, Air pollution control: The evaluation of TerphApm@MWCNTs as a novel heterogeneous sorbent for benzene removal from air by solid phase gas extraction, Arab. J. Chem., 13 (2020) 1741–1751. https://doi.org/10.1016/j.arabjc.2018.01.011

[5] J. Rakhtshah, H. Shirkhanloo, N. Esmaeili, A rapid extraction of toxic styrene from water and wastewater samples based on hydroxyethyl methylimidazolium tetrafluoroborate immobilized on MWCNTs by ultra-assisted dispersive cyclic conjugation-micro-solid phase extraction, Microchem. J., 170 (2021) 106759. https://doi.org/ 10.1016/j.microc.2021.106759

[6] S. Arellano-Cárdenas, S. López-Cortez, M. Cornejo-Mazón, J. C. Mares-Gutiérrez, Study of malachite green adsorption by organically modified clay using a batch method, Appl.

Surf. Sci., 280 (2013) 74–78. https://doi.org/10.1016/j.apsusc.2013.04.097

[7] K. Vasanth Kumar, S. Sivanesan, V. Ramamurthi, Adsorption of malachite green onto Pithophora sp., a fresh water algae: Equilibrium and kinetic modelling, Process Biochem., 40 (2005) 2865–2872. https://doi.org/ 10.1016/j.procbio.2005.01.007

[8] A. Dehbi, Comparative study of malachite green and phenol adsorption on synthetic hematite iron oxide nanoparticles (α-Fe2O3), Surf. Interface., 21 (2020) 100637. https://doi.org/ 10.1016/j.surfin.2020.100637

[9] M. Mohammadi Asl, N. Mansouri, S. A. R. Haji Seyed Mirzahosseini, F. Atabi, Simultaneity comparative evaluation of toluene removal from the air by adsorption and UV semi-degradation-based adsorption procedure, Int. J. Environ. Sci. Technol., 21 (2024) 6677-6694. https://doi.org/10.1007/s13762-024-05503-0

[10] M. M. Asl, F. Atabi, Functionalized graphene oxide with bismuth and titanium oxide nanoparticles for efficiently removing formaldehyde from the air by photocatalytic degradation–adsorption process, J. Anal. Test., 7 (2023) 444-458. https://doi.org/10.1007/s41664-023-00272-0

[11] R. Ashouri, Dynamic and static removal of benzene from air based on task-specific ionic liquid coated on MWCNTs by sorbent tube-headspace solid-phase extraction procedure, Int. J. Environ. Sci. Technol., 18 (2021) 2377-2390. https://doi.org/10.1007/s13762-020-02995-4

[12] S. Teimoori, H. Shirkhanloo, A. H. Hassani, M. Panahi, N. Mansouri, New extraction of toluene from water samples based on nano-carbon structure before determination by gas chromatography, Int. J. Environ. Sci. Technol., 20 (2023) 6589–6608. https://doi.org/ 10.1007/s13762-023-04906-9

[13] A. Faghihi-Zarandi, H. Shirkhanloo, C. Jamshidzadeh, A new method for removal of hazardous toluene vapor from air based on ionic liquid-phase adsorbent, Int. J. Environ. Sci. Technol., 16 (2019) 2797–2808. https://doi.org/ 10.1007/s13762-018-1975-5

[14] A. Faghihi-Zarandi, J. Rakhtshah, B. Bahrami Yarahmadi, A rapid removal of xylene vapor from environmental air based on bismuth oxide coupled to heterogeneous graphene/graphene oxide by UV photo-catalectic degradation-adsorption procedure, J. Environ. Chem. Eng., 8 (2020) 104193. https://doi.org/ 10.1016/j.jece.2020.104193

[15] R. F. Wang, L. G. Deng, K. Li, X. J. Fan, W. Li, H. Q. Lu, Fabrication and characterization of sugarcane bagasse–calcium carbonate composite for the efficient removal of crystal violet dye from wastewater, Ceram. Int., 46 (2020) 27484–27492. https://doi.org/ 10.1016/j.ceramint.2020.07.237

[16] I. Loulidi, Adsorptive removal of chromium (VI) using walnut shell, almond shell, coconut shell and peanut shell, Res. J. Chem. Environ., 23 (2019) 25–32. http://www.scopus.com/inward/record.url?eid=2-s2.0-85081283619&partnerID=MN8TOARS

[17] M. El Khomri, N. El Messaoudi, A. Dbik, S. Bentahar, A. Lacherai, Efficient adsorbent derived from Argania Spinosa for the adsorption of cationic dye: Kinetics, mechanism, isotherm and thermodynamic study, Surf. Interface., 20 (2020) 100601. https://doi.org/ 10.1016/j.surfin.2020.100601

[18] M. A. Fawzy, Sustainable use of marine Macroalga Sargassum muticum as a biosorbent for hazardous crystal violet dye: Isotherm, kinetic and thermodynamic modeling, Sustain., 15 (2023) 15064. https://doi.org/ 10.3390/su152015064

[19] N. Ameram, Chemical composition in sugarcane bagasse: Delignification with sodium hydroxide, Malaysian J. Fundam. Appl. Sci., 15 (2019) 232–236. https://doi.org/ 10.11113/mjfas.v15n2.1118

[20] T. L. Bezerra, A. J. Ragauskas, A review of sugarcane bagasse for second-generation bioethanol and biopower production, Biofuel. Bioprod. Bior., 10 (2016) 634–647. https://doi.org/ 10.1002/bbb.1662

[21] V. Yogeshwaran, A. K. Priya, Experimental studies on the removal of heavy metal ion concentration using sugarcane bagasse in batch adsorption process, Desalin. Water Treat., 224 (2021) 256–272. https://doi.org/ 10.5004/dwt.2021.27160

[22] H. Tahir, M. Sultan, N. Akhtar, U. Hameed, T. Abid, Application of natural and modified sugar cane bagasse for the removal of dye from aqueous solution, J. Saudi Chem. Soc., 20 (2016) S115–S121. https://doi.org/ 10.1016/j.jscs.2012.09.007

[23] E. K. Guechi, O. Hamdaoui, Biosorption of methylene blue from aqueous solution by potato (Solanum tuberosum) peel : equilibrium modelling, kinetic, and thermodynamic study, Desalin. Water Treat., 57 (2016) 10270-10285. https://doi.org/10.1080/19443994.2015.1035338

[24] I. Loulidi, Adsorption of crystal violet onto an agricultural waste residue: Kinetics, isotherm, thermodynamics, and mechanism of adsorption, Sci. World J., 2020 (2020) 873521. https://doi.org/ 10.1155/2020/5873521

[25] K. D. Belaid, S. Kacha, Study of the kinetics and thermodynamics of the adsorption of a basic dye on sawdust, J. Water Sci., 24 (2011)131–144. https://doi.org/ 10.7202/1006107ar

[26] E. Sudova, J. Machova, Z. Svobodova, T. Vesely, Negative effects of malachite green and possibilities of its replacement in the treatment of fish eggs and fish: A review, Vet. Med., 52 (2007) 527–539. https://doi.org/ 10.17221/2027-VETMED

[27] M. Sadoq, Elimination of crystal violet from aqueous solution by adsorption on naturel polysaccharide: Kinetic, isotherm, thermodynamic studies and mechanism analysis, Arab. J. Chem., 17 (2024) 105453. https://doi.org/ 10.1016/j.arabjc.2023.105453

[28] B. Shetty, Y. S. R, J. Johns, A Green approach to the removal of Malachite Green dye from aqueous medium using chitosan/cellulose blend, Res. Square, 2022. https://doi.org/ 10.21203/rs.3.rs-1376666/v2

[29] S. Dawood, T. K. Sen, Removal of anionic dye Congo red from aqueous solution by raw pine and acid-treated pine cone powder as adsorbent: Equilibrium, thermodynamic, kinetics, mechanism and process design, Water Res., 46 (2012) 1933–1946. https://doi.org/ 10.1016/j.watres.2012.01.009

[30] D. Kavitha, C. Namasivayam, Experimental and kinetic studies on methylene blue adsorption by coir pith carbon, Bioresour. Technol., 98 (2007) 14–21. https://doi.org/ 10.1016/j.biortech.2005.12.008

[31] M. Ertaş, M. Hakki Alma, Pyrolysis of laurel (Laurus nobilis L.) extraction residues in a fixed-bed reactor: Characterization of bio-oil and bio-char, J. Anal. Appl. Pyrolysis, 88 (2010) 22–29. https://doi.org/ 10.1016/j.jaap.2010.02.006

[32] A. Kali, Efficient adsorption removal of an anionic azo dye by lignocellulosic waste material and sludge recycling into combustible briquettes, Colloids Interfaces, 6 (2022) 22. https://doi.org/ 10.3390/colloids6020022

[33] A. F. Abbas, M. J. Ahmed, Mesoporous activated carbon from date stones (Phoenix dactylifera L.) by one-step microwave assisted K_2CO_3 pyrolysis, J. Water Process Eng., 9 (2016) 201–207. https://doi.org/ 10.1016/j.jwpe.2016.01.004

[34] Z. Belala, M. Jeguirim, M. Belhachemi, F. Addoun, G. Trouvé, Biosorption of basic dye from aqueous solutions by date stones and palm-trees waste: Kinetic, equilibrium and thermodynamic studies, Desalin., 271 (2011) 80–87. https://doi.org/ 10.1016/j.desal.2010.12.009

[35] N. El Messaoudi, M. El Khomri, S. Bentahar, A. Dbik, A. Lacherai, B. Bakiz, Evaluation of performance of chemically treated date stones: Application for the removal of cationic dyes from aqueous solutions, J. Taiwan Inst. Chem. Eng., 67 (2016) 244–253. https://doi.org/ 10.1016/j.jtice.2016.07.024

[36] M. A. Al-Ghouti, J. Li, Y. Salamh, N. Al-Laqtah, G. Walker, M. N. M. Ahmad, Adsorption mechanisms of removing heavy

metals and dyes from aqueous solution using date pits solid adsorbent, J. Hazard. Mater., 176 (2010) 510–520. https://doi.org/ 10.1016/j.jhazmat.2009.11.059

[37] L. Rodier, K. Bilba, C. Onésippe, M. A. Arsène, Utilization of bio-chars from sugarcane bagasse pyrolysis in cement-based composites, Ind. Crops Prod., 141 (2019) 111731. https://doi.org/ 10.1016/j.indcrop.2019.111731

[38] E. N. Bakatula, D. Richard, C. M. Neculita, G. J. Zagury, Determination of point of zero charge of natural organic materials, Environ. Sci. Pollut. Res., 25 (2018) 7823–7833. https://doi.org/ 10.1007/s11356-017-1115-7

[39] K. M. Kifuani, Adsorption d'un colorant basique, Bleu de Méthylène, en solution aqueuse, sur un bioadsorbant issu de déchets agricoles de Cucumeropsis mannii Naudin, Int. J. Biol. Chem. Sci., 12 (2018) 558. https://doi.org/ 10.4314/ijbcs.v12i1.43

[40] E. K. Guechi, O. Hamdaoui, Biosorption of methylene blue from aqueous solution by potato (Solanum tuberosum) peel: equilibrium modelling, kinetic, and thermodynamic studies, Desalin. Water Treat., 57 (2016) 10270–10285. https://doi.org/ 10.1080/19443994.2015.1035338

[41] N. B. Singh, G. Nagpal, S. Agrawal, Water purification by using adsorbents : A review, Environ. Technol. Innov., 11 (2018) 187–240. https://doi.org/ 10.1016/j.eti.2018.05.006

[42] S. D. Ahranjani, A lead analysis based on amine-functionalized bimodal mesoporous silica nanoparticles in human biological samples by ultrasound assisted-ionic liquid trap-micro solid phase extraction, J. Pharm. Biomed. Anal., 157 (2018) 1-9. https://doi.org/10.1016/j.jpba.2018.05.004

[43] Z. Khademi, B. Ramavandi, M. T. Ghaneian, The behaviors and characteristics of a mesoporous activated carbon prepared from Tamarix hispida for Zn(II) adsorption from wastewater, J. Environ. Chem. Eng., 3 (2015) 2057–2067. https://doi.org/ 10.1016/j.jece.2015.07.012

[44] F. Wu, R. Tseng, S. Huang, R. Juang, Characteristics of pseudo-second-order kinetic model for liquid-phase adsorption : A mini-review, Chem. Eng. J., 151 (2009) 1–9. https://doi.org/ 10.1016/j.cej.2009.02.024

[45] S. Sahu, Adsorption of methylene blue on chemically modified lychee seed biochar: Dynamic, equilibrium, and thermodynamic study, J. Mol. Liq., 315 (2020) 113743. https://doi.org/ 10.1016/j.molliq.2020.113743

[46] H. Zeghache, S. Hafsi, N. Gherraf, Adsorption of organic dyes onto commercial activated carbon by using non-linear regression method, Environ. Asia, 12 (2019) 127–142. https://doi.org/ 10.14456/ea.2019.15

[47] P. Sampranpiboon, Equilibrium isotherm models for adsorption of zinc (II) ion from aqueous solution on pulp waste faculty of engineering, WSEAS Trans. Environ. Dev., 10 (2014) 35–47. https://wseas.org/cms.action?id=4031